LETTER

doi:10.1038/nature11418

Stabilization of Leidenfrost vapour layer by textured superhydrophobic surfaces

Ivan U. Vakarelski[1,2], Neelesh A. Patankar[3], Jeremy O. Marston[1], Derek Y. C. Chan[4,5] & Sigurdur T. Thoroddsen[1,2]

In 1756, Leidenfrost[1] observed that water drops skittered on a sufficiently hot skillet, owing to levitation by an evaporative vapour film. Such films are stable only when the hot surface is above a critical temperature, and are a central phenomenon in boiling[2]. In this so-called Leidenfrost regime, the low thermal conductivity of the vapour layer inhibits heat transfer between the hot surface and the liquid. When the temperature of the cooling surface drops below the critical temperature, the vapour film collapses and the system enters a nucleate-boiling regime, which can result in vapour explosions that are particularly detrimental in certain contexts, such as in nuclear power plants[3]. The presence of these vapour films can also reduce liquid–solid drag[4–6]. Here we show how vapour film collapse can be completely suppressed at textured superhydrophobic surfaces. At a smooth hydrophobic surface, the vapour film still collapses on cooling, albeit at a reduced critical temperature, and the system switches explosively to nucleate boiling. In contrast, at textured, superhydrophobic surfaces, the vapour layer gradually relaxes until the surface is completely cooled, without exhibiting a nucleate-boiling phase. This result demonstrates that topological texture on superhydrophobic materials is critical in stabilizing the vapour layer and thus in controlling—by heat transfer—the liquid–gas phase transition at hot surfaces. This concept can potentially be applied to control other phase transitions, such as ice or frost formation[7–9], and to the design of low-drag surfaces at which the vapour phase is stabilized in the grooves of textures without heating[10].

Heat transfer and boiling on a heated solid surface in contact with liquid are familiar phenomena observed in our daily lives, and occur in many industrial processes. As the vessel containing a liquid is progressively heated, the liquid will start to boil, with vapour bubbles forming at the hot surface. This is the nucleate-boiling regime. If the surface temperature is increased further, a continuous vapour film will form that leads to the film-boiling or Leidenfrost regime. It is known that surface properties such as roughness and wettability can alter the transition temperature from the nucleate-boiling to the film-boiling regime[11–16]. As the low thermal conductivity of the vapour layer dramatically reduces the efficiency of heat transfer, the traditional focus is to increase the temperature at which film boiling occurs[13]. However, if the vapour layer is to be used for drag reduction[4–6,17–20], lowering the temperature of film boiling is beneficial, as the presence of a Leidenfrost vapour layer can reduce the hydrodynamic drag force on a heated sphere moving in liquid by up to 85%[6].

Takata *et al.*[12] have reported that the initiation of nucleate boiling can be suppressed at what they termed "super-water-repellent" surfaces. Here we show that a textured superhydrophobic surface can eliminate the collapse of the vapour film, thus making it possible to maintain a stable vapour film at all temperatures above the boiling point of the liquid—that is, at all superheats. To this end, we investigated cooling and heating phenomena of heated surfaces that possess different degrees of hydrophobicity in water.

In our cooling experiments we use 20-mm-diameter stainless-steel spheres, and in our heating experiments 24-mm-diameter stainless-steel cylinders and stainless-steel vessels (capacity 60 ml). The stainless-steel surfaces are modified to have superhydrophilic, hydrophilic, hydrophobic or superhydrophobic wetting properties, as characterized by water-drop contact angle in air. Hydrophilic surfaces were produced by cleaning the steel surface with organic reagents, resulting in water contact angles of $<30^\circ$. Hydrophobic surfaces were produced by silanization with trichloro(1H,1H,2H,2H-perfluorooctyl)silane, giving contact angles of $\sim 100^\circ$. Superhydrophobic surfaces with water contact angles of $>160^\circ$ were produced by treatment with a commercial coating agent (Glaco Mirror Coat 'Zero', Soft 99 Co.) containing nanoparticles and organic reagent. Superhydrophilic surfaces, with contact angles of $<10^\circ$, were produced from the superhydrophobic surface by plasma cleaning to remove the organic coating, while retaining the same texture and geometric morphology (see Supplementary Information for details).

Figure 1a is an atomic-force micrograph of the superhydrophobic surface coating, showing its rough surface topography. The very high contact angle subtended by a superhydrophobic sphere at the air–water meniscus is shown in Fig. 1b. When the sphere is fully immersed in water, its surface has a silver, mirror-like sheen, caused by reflection from the thin air layer retained on the surface. This is a signature of the Cassie state[21–24], in which water is in physical contact only with the roughness peaks created by the coating (Fig. 1c). This type of air entrapment, called plastron, has been shown to reduce hydrodynamic drag on spheres moving in water[20], and is used by some aquatic insects to facilitate underwater breathing[25].

We study the cooling of superhydrophilic, hydrophilic, hydrophobic and superhydrophobic spheres that have been pre-heated in a temperature-controlled furnace and then immersed in a glass tank filled with water at 22 °C (Supplementary Fig. 4). The state of the water at the sphere surface during subsequent cooling is captured on high-speed video, and the sphere temperature is monitored by an inserted thermocouple-probe thermometer. The progress of the cooling events for the hydrophilic, hydrophobic and superhydrophobic spheres can be seen in Supplementary Movies 1, 2 and 3, respectively. The superhydrophilic and hydrophilic spheres were heated to a maximum temperature of 700 °C, but the maximum temperature to which the hydrophobic and superhydrophobic spheres could be raised was limited to ~400 °C by the thermal stability of the organic coating. For the superhydrophilic sphere, the maximum temperature was not high enough to initiate film boiling; when the sphere came into contact with the water, it cooled almost instantaneously, accompanied by a vigorous release of bubbles. For all other surfaces, the initial sphere temperatures were high enough to be in the film-boiling regime, in which a continuous vapour layer coated the spheres, with a single bubble dome formed on the top of the sphere by buoyancy effects. During the initial stage of cooling, the bubble dome would grow and

[1]Division of Physical Sciences and Engineering, King Abdullah University of Science and Technology (KAUST), Thuwal 23955-6900, Saudi Arabia. [2]Clean Combustion Research Center, King Abdullah University of Science and Technology (KAUST), Thuwal 23955-6900, Saudi Arabia. [3]Department of Mechanical Engineering, Northwestern University, 2145 Sheridan Road, B224, Evanston, Illinois 60208–3111, USA. [4]Department of Mathematics and Statistics, University of Melbourne, Parkville 3010, Victoria, Australia. [5]Faculty of Life and Social Sciences, Swinburne University of Technology, Hawthorn 3122, Victoria, Australia.

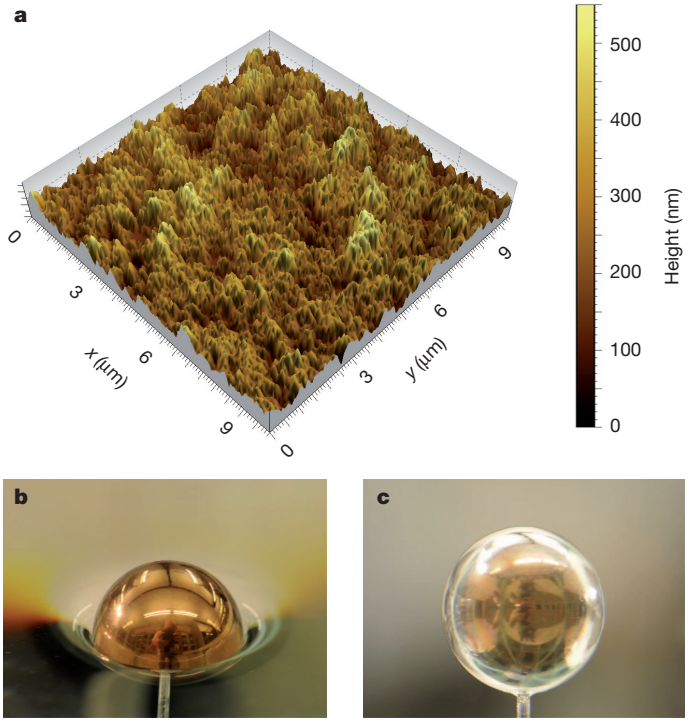

Figure 1 | Surface topography and images of the superhydrophobic sphere. **a**, Three-dimensional representation of an atomic-force micrograph of a 10-μm^2 region of the superhydrophobic surface coating. The combination of high surface roughness with an organic coating provides a high water contact angle, of >160°. **b**, Image of the superhydrophobic sphere held on the water surface, showing the high contact angle. **c**, Image of the superhydrophobic sphere immersed in water. The silver-mirror sheen of the immersed sphere is due to a thin air layer retained on the sphere surface, and is the signature appearance of a Cassie state of the water adjacent to the surface. See Supplementary Information for further details of the preparation and characterization of the superhydrophobic coating (Supplementary Figs 1, 2).

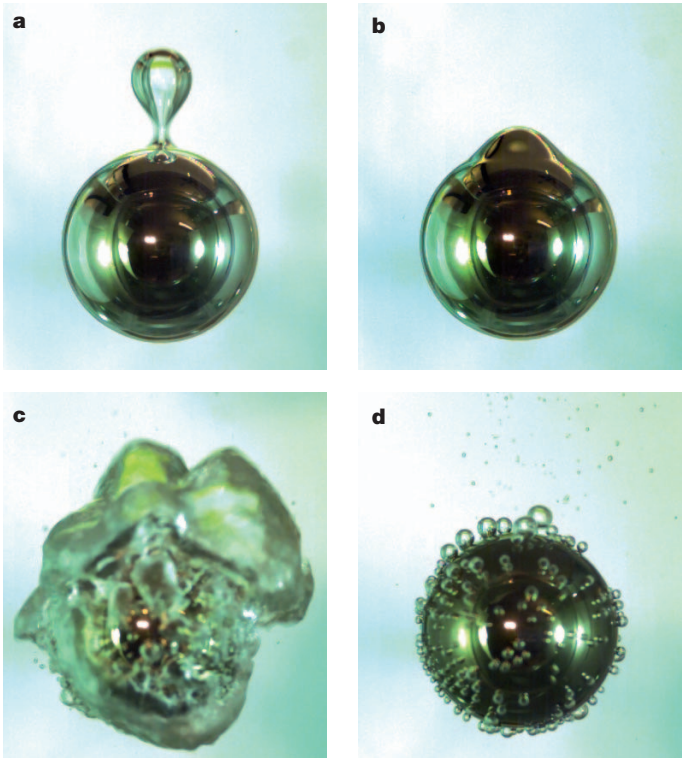

Figure 2 | High-speed camera snapshots of 20-mm steel spheres cooling in water. **a**, Bubble pinch-off from the vapour dome of a hot, superhydrophobic sphere cooling in the Leidenfrost regime. Water pool temperature is 100 °C; sphere temperature is T_s = 200 °C. **b**, Final state of the same superhydrophobic sphere, cooled to the pool temperature (T_s = 100 °C). **c, d**, Hydrophilic sphere cooling in water at 100 °C, at the moment of the explosive transition from film boiling to nucleate boiling (**c**, T_s = 275 °C) and during nucleate boiling (**d**, T_s = 200 °C). Sphere cooling events in water at 22 °C are shown in Supplementary Movies 1 (hydrophilic sphere), 2 (hydrophobic sphere) and 3 (superhydrophobic sphere). Supplementary Movie 4 shows hydrophilic and superhydrophobic spheres cooling in water at 100 °C.

pinch off periodically (Fig. 2a). On further cooling, the film-boiling mode on the hydrophilic sphere ended with collapse of the vapour layer, marked by an explosive release of bubbles (Fig. 2c). This was followed by a short phase of rapid cooling in the nucleate-boiling mode (Fig. 2d). Film boiling on the hydrophobic sphere also ended with an almost instantaneous collapse of the vapour layer. However, for the superhydrophobic sphere no vapour-layer collapse was observed. Instead, the vapour layer gradually relaxed over the entire sphere surface, and when cooling was complete a residual bubble dome remained on the sphere apex (Fig. 2b), and the sphere surface exhibited the silver sheen indicative of a final Cassie state of the liquid adjacent to the sphere surface (Supplementary Fig. 3).

Figure 3 shows the measured sphere temperature plotted against the immersion time. The superhydrophilic sphere (Fig. 3a) begins its cooling in the nucleate-boiling regime, and its temperature drops rapidly to the pool temperature. The cooling of the hydrophilic (Fig. 3a) and hydrophobic (Fig. 3b) spheres begins in the Leidenfrost film-boiling regime. In both cases, the vapour layer collapses at the Leidenfrost point, indicated by a sharp increase in cooling rate at ~420 °C for the hydrophilic sphere, and at ~210 °C for the hydrophobic sphere. However, for the superhydrophobic sphere, film boiling is maintained down to the pool temperature (22 °C) without vapour-layer collapse and transition to nucleate boiling (Fig. 3b).

Cooling experiments at elevated water pool temperatures of 80 and 100 °C confirmed the same trends as the room-temperature cooling experiments, with respect to the sphere hydrophobicity (Supplementary Fig. 5 and Supplementary Movie 4). In fact, as long as the water contact angle at room temperature exceeded 140°, achievable at textured superhydrophobic surfaces, no Leidenfrost transition was observed (Supplementary Figs 7, 8).

We performed heating experiments to further characterize surface properties at the boiling transition. A cartridge heater placed inside a stainless-steel cylinder (Fig. 4a and Supplementary Fig. 9) was immersed in a water-filled beaker sitting on a hot plate that heated the water to slow boiling, T_w = 100 °C. The surface temperature of the cylinder, T_s, was measured with an inserted thermocouple at constant heat flux, by controlling the applied power to the heater. We acquired high-speed video sequences along with the temperature measurements.

Figure 4d shows the measured variations of heat flux with surface temperature at steady state for the four types of surface wettability. As expected for the low values of heat flux used here, the heat exchange occurred in the nucleate-boiling regime (Fig. 4b and Supplementary Fig. 13) for the superhydrophilic and hydrophilic surfaces. However, as in the sphere-cooling experiments, the superhydrophobic surface was able to sustain a vapour layer in the Leidenfrost regime for all surface superheats. This is readily observed in both the appearance of the vapour layer and the magnitude of the increase in surface temperature with increasing heat flux (Fig. 4d).

When the temperature of the superhydrophobic cylinder was in equilibrium with the ambient water ($T_s = T_w$ = 100 °C), the cylinder's surface appeared smooth and shiny. With increasing heater power, the appearance of surface ripples[6] accompanied a gradual transition to the Leidenfrost regime (Fig. 4c, Supplementary Fig. 10 and Supplementary Movie 5). Additional experiments with the immersion heater (see Supplementary Fig. 11) showed that for the superhydrophobic surface there was no hysteresis between heating and cooling experiments.

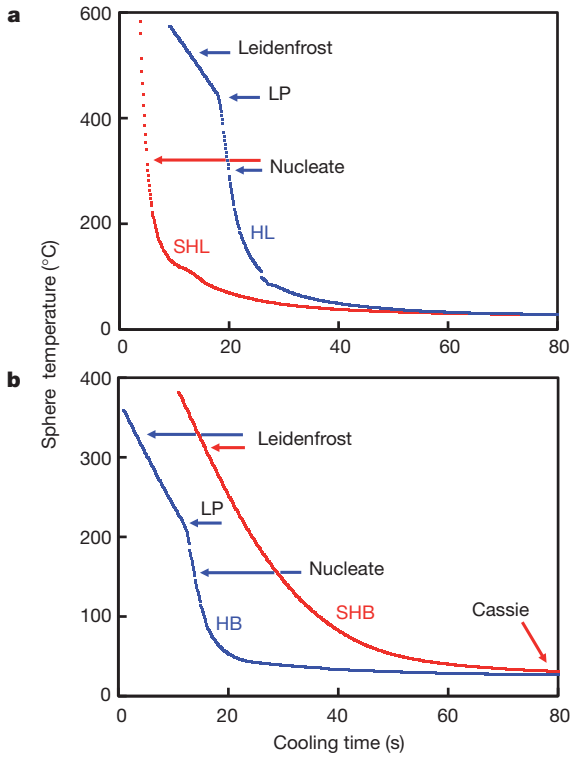

Figure 3 | Sphere temperature versus cooling time for 20-mm steel spheres held in water at 22 °C. a, Superhydrophilic sphere (contact angle <10°, SHL) and hydrophilic sphere (contact angle ~30°, HL). **b**, Hydrophobic sphere (contact angle ~100°, HB) and superhydrophobic surface sphere (contact angle >160°, SHB). Arrows indicate the Leidenfrost film-boiling regime, Leidenfrost-point transition (LP) and nucleate-boiling regime. The Leidenfrost transition in the superhydrophilic case occurs above the maximum temperature shown in the figure. In the superhydrophobic case, the Leidenfrost state relaxes to the Cassie state without passing through the nucleate-boiling regime.

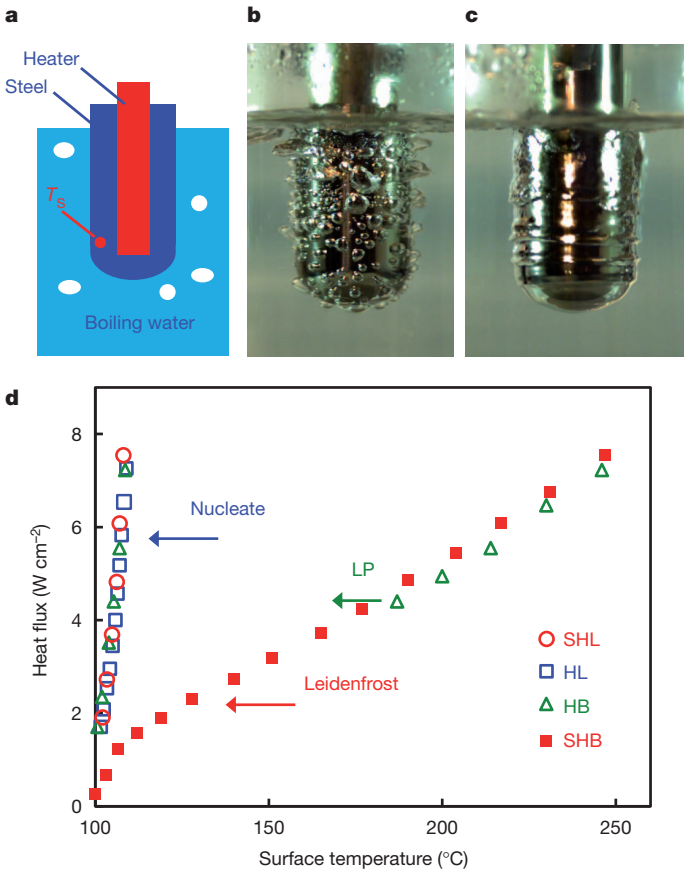

Figure 4 | Surface temperature versus heat flux in heating experiments. **a**, Schematics of the immersion heater. **b**, **c**, High-speed camera snapshots of the heater in boiling (100 °C) water for the case of (**b**) hydrophobic surface in the nucleate-boiling regime, at surface temperature $T_s = 106$ °C; and (**c**) superhydrophobic surface in the Leidenfrost regime, $T_s = 210$ °C. **d**, Dependence of the heat flux on the heater surface temperature for four types of surface in the nucleate-boiling and Leidenfrost film-boiling regimes. Abbreviations as in Fig. 3.

Keeping the surface immersed in water for up to 24 hours did not alter the smooth transition to the Leidenfrost regime (Supplementary Fig. 11). Although in such cases the surfaces appeared matte instead of shiny, suggesting that the vapour layer was not in a pure Cassie state, on heating, they returned smoothly to the Leidenfrost state (Supplementary Fig. 12). The same recovery property of superhydrophobic surfaces has been demonstrated recently using electrophoresis[26].

For the hydrophobic surface, it was possible to maintain the Leidenfrost vapour regime only if the cylinder was overheated before immersion to ~350 °C, and the heater power was maximized on immersion. When the surface temperature was allowed to fall below ~170 °C, the Leidenfrost vapour layer collapsed, and the switched to the nucleate-boiling branch (Fig. 4d).

Experiments with a stainless-steel cup placed on a hot plate showed the same behaviour as with the immersion heater (Supplementary Figs 14, 15). The good agreement among the cooling experiments and the two types of heating experiment confirm the geometry-independence and universality of the superhydrophobic surface effect in stabilizing the Leidenfrost vapour layer (compare Fig. 4d with Supplementary Figs 6 and 15).

By combining results for cooling experiments at constant initial heat content and high initial temperatures, and heating experiments at constant heating power but over a range of lower superheat temperatures, we have shown that the mode of heat transfer at the solid–liquid interface can be controlled by a combination of the surface morphology and surface chemistry of the solid surface. The observations for the hydrophilic and the hydrophobic surfaces are consistent with the standard transition between nucleate and film boiling[27]. The strong effect of the superhydrophilic surface in increasing the Leidenfrost temperature and enhancing boiling heat transfer has also been investigated recently[13]. However, we now show that for textured superhydrophobic surfaces the heat exchange always occurs in the presence of a Leidenfrost vapour layer, within the film-boiling regime. This behaviour has not been observed previously and represents a significant departure from the characteristic form of the classical boiling heat-transfer curve[10,28,29] of heat flux versus surface superheat temperature. The currently accepted form of the boiling curve comprises a critical heat-flux maximum and a Leidenfrost-point minimum that characterizes the transition between nucleate and film boiling. But at a textured superhydrophobic surface, the heat flux is a smoothly increasing function of superheat temperature, owing to the vapour layer that is always maintained at such surfaces (Supplementary Fig. 17).

The vapour layer on the superhydrophobic surface is sustained by the high surface roughness and porosity, coupled with the intrinsic, non-wetting hydrophobicity due to surface chemical treatment. These are the requisite conditions for the existence of a large non-wetting vapour layer (see Supplementary Information discussion on stabilization of vapour layers due to texture, and Supplementary Figs 18, 19). Furthermore, the three-dimensional nature of the surface roughness permits only small areas of direct contact between the peaks of the rough surface and the liquid interface. Contributions to the total heat transfer by such small areas are thus limited, and any onset of heterogeneous nucleation of bubbles will simply be taken up in the surface vapour layer that in effect will contribute to a smooth transition to the Leidenfrost regime. These conclusions are in complete accord with

what we found when repeating Leidenfrost's experiments[1] of drop evaporation at heated surfaces. For hydrophobic surfaces we observed the classical transition from nucleate to film-boiling mode, whereas at superhydrophobic surfaces nucleate boiling is absent at all superheats (Supplementary Fig. 16).

Although it has been demonstrated that the stability of the vapour layer in Leidenfrost drop experiments is sensitive to external perturbations such as vibrations, cooling rate and internal fluid circulation within the drops[31], and the hypothesis has been advanced that when the fluid drop contact angle at the surface attains the limiting value of 180°, the film-boiling regime might be possible at all superheat temperatures[32], this study has demonstrated that with the combination of surface roughness and chemical modifications Leidenfrost vapour layer stability and the film-boiling behaviour are readily achievable and remain robust under general operational conditions.

With the recent development of a wide variety of laboratory-designed and commercially available textured surface coatings with superhydrophobic[23,24], superamphiphobic[8,9], anti-frost[7] or switchable-hydrophobicity[30] properties, the effect on thermal exchange shown here opens possibilities for new applications of such coatings, ranging from the design of efficient heat-exchange devices to technologies for aqueous drag reduction.

METHODS SUMMARY

In cooling experiments we used 20-mm-diameter stainless-steel spheres (FRITSCH GmbH). In heating experiments we used an immersion heater or a 60-ml stainless-steel cup. The immersion heater is a 24-mm-diameter stainless-steel hollow cylinder with an electric heater cartridge fitted inside. All stainless-steel surfaces are modified as follows. Smooth hydrophilic surfaces are produced by cleaning with organic reagents. Smooth hydrophobic surfaces are produced by silanization with trichloro(1H,1H,2H,2H-perfluorooctyl)silane. Textured superhydrophobic surfaces are produced by treatment with a commercial superhydrophobic coating agent (Glaco Mirror Coat 'Zero', Soft 99 Co.). Textured superhydrophilic surfaces are produced by plasma cleaning of the surfaces previously treated with the superhydrophobic agent. A 2-mm hole is drilled into the spheres, the immersion-heater cylinder wall or the bottom of the cup vessel to allow the insertion of a thermocouple probe to measure the surface temperature. In cooling experiments, the heated sphere is quenched in a water-filled vessel and the sphere temperature is recorded as function of time. In heating experiments, the cylindrical heater is immersed in a water-filled glass beaker placed on a hot plate to control the water temperature, and the heater surface temperature is measured as a function of the applied power to the heater cartridge in the cylinder. The heat transfer process on the sphere surface or the immersion-heater surface is recorded using a high-speed video camera (Photron Fastcam SA-5). In the cup vessel experiments, the water-filled cup is placed on a hot plate and the vessel surface temperature is measured as a function of the hot-plate temperature. The same setup is used to measure the evaporation time of water droplets placed on the bottom of the cup. Further details of methods are available in Supplementary Information.

Received 11 February; accepted 18 July 2012.

1. Leidenfrost, J. G. *De aquae communis nonnullis qualitatibus tractatus* (Duisburg, 1756); transl. Wares, C. On the fixation of water in diverse fire. *Int. J. Heat Mass Transfer* **9,** 1153–1166 (1966).
2. Bernardin, J. D. & Mudawar, I. The Leidenfrost point: experimental study and assessment of existing models. *Trans. Am. Soc. Mech. Eng.* **121,** 894–903 (1999).
3. Berthoud, G. Vapor explosions. *Annu. Rev. Fluid Mech.* **32,** 573–611 (2000).
4. Linke, H. *et al.* Self-propelled Leidenfrost droplets. *Phys. Rev. Lett.* **96,** 154502 (2006).
5. Lagubeau, N., Le Merrer, M., Clanet, C. & Quéré, D. Leidenfrost on a ratchet. *Nature Phys.* **7,** 395–398 (2011).
6. Vakarelski, I. U., Marston, J. O., Chan, D. Y. C. & Thoroddsen, S. T. Drag reduction by Leidenfrost vapor layers. *Phys. Rev. Lett.* **106,** 214501 (2011).
7. Mishchenko, L. *et al.* Design of ice-free nanostructured surfaces based on repulsion of impacting water droplets. *ACS Nano* **4,** 7699–7707 (2010).
8. Wong, T. S. *et al.* Bioinspired self-repairing slippery surfaces with pressure-stable omniphobicity. *Nature* **477,** 443–447 (2011).
9. Deng, X. Mammen, L. Butt, H. J. & Vollmer, D. Candle soot as a template for a transparent robust superamphiphobic coating. *Science* **335,** 67–70 (2012).
10. Patankar, N. A. Supernucleating surfaces for nucleate boiling and dropwise condensation heat transfer. *Soft Matter* **6,** 1613–1620 (2010).
11. Wang, C. H. & Dhir, V. K. Effect of surface wettability on active nucleation site density during pool boiling of water on a vertical surface. *J. Heat Transfer* **115,** 659–669 (1993).
12. Takata, Y., Hidaka, S. & Kohno, M. in *Proc. Fifth Intl Conf. Enhanced, Compact and Ultra-compact Heat Exchangers: Science, Engineering and Technology* (eds Shah, R. K. *et al.*) 300–304 (Engineering Conferences International, 2005).
13. Chen, R. *et al.* Nanowires for enhanced boiling heat transfer. *Nano Lett.* **9,** 548–553 (2009).
14. Liu, G. & Craig, V. S. J. Macroscopically flat and smooth superhydrophobic surfaces: heating induced wetting transitions up to the Leidenfrost temperature. *Faraday Discuss.* **146,** 141–151 (2010).
15. Liu, G., Fu, L., Rode, A. V. & Craig, V. S. J. Water droplet motion control on superhydrophobic surfaces: exploiting the Wenzel-to-Cassie transition. *Langmuir* **27,** 2595–2600 (2011).
16. Kim, H., Truong, B., Buongiomo, J. & Hu, L. On the effect of surface roughness height, wettability, and nanoporosity on Leidenfrost phenomena. *Appl. Phys. Lett.* **98,** 083121 (2011).
17. Zvirin, Y., Hewitt, G. R. & Kenning, D. B. R. Boiling on free-falling spheres: drag and heat transfer coefficients. *Exp. Heat Transf.* **3,** 185–214 (1990).
18. Rothstein, J. P. Slip on superhydrophobic surfaces. *Annu. Rev. Fluid Mech.* **42,** 89–109 (2010).
19. Ceccio, S. L. Friction drag reduction of external flows with bubble and gas injection. *Annu. Rev. Fluid Mech.* **42,** 183–203 (2010).
20. McHale, G., Newton, M. I. & Shirtcliffe, N. J. Immersed superhydrophobic surfaces: gas exchange, slip and drag reduction properties. *Soft Matter* **6,** 714–719 (2010).
21. Cassie, A. B. D. & Baxter, S. Wettability of porous surfaces. *Trans. Faraday Soc.* **40,** 0546–0550 (1944).
22. Patankar, N. A. On the modeling of hydrophobic contact angles on rough surfaces. *Langmuir* **19,** 1249–1253 (2003).
23. Larmour, I. A., Bell, S. E. J. & Saunders, G. S. Remarkably simple fabrication of superhydrophobic surfaces using electroless galvanic deposition. *Angew. Chem. Int. Edn Engl* **46,** 1710–1712 (2007).
24. Quéré, D. Wetting and roughness. *Annu. Rev. Mater. Res.* **38,** 71–99 (2008).
25. Flynn, M. R. & Bush, J. W. M. Underwater breathing: the mechanics of plastron respiration. *J. Fluid Mech.* **608,** 275–296 (2008).
26. Lee, C. & Kim, C.-J. Underwater restoration and retention of gases on superhydrophobic surfaces for drag reduction. *Phys. Rev. Lett.* **106,** 014502 (2011).
27. Dhir, V. K. & Purohit, G. P. Subcooled film boiling heat transfer from spheres. *Nucl. Eng. Des.* **47,** 49–66 (1978).
28. Nukiyama, S. Maximum and minimum values of heat Q transmitted from metal to boiling water under atmospheric pressure. *J. Jpn Soc. Mech. Engrs* **37,** 367–374 (1934).
29. Witte, L. C. & Lienhard, J. H. On the existence of two "transition" boiling cure. *Int. J. Heat Mass Transf.* **25,** 771–779 (1982).
30. Celestini, F. & Kirstetter, G. Effect of an electric field on a Leidenfrost droplet. *Soft Matter* **8,** 5992–5995 (2012).
31. Baumeister, K. J., Hendricks, R. C. & Hamill, T. D. *Metastable Leidenfrost States* (NASA Technical Note D3226, 1966).
32. Carey, V. P. in *Liquid-Vapor Phase-Change Phenomena* 2nd edn 353–356 (Taylor and Francis, 2008).

Supplementary Information is available in the online version of the paper.

Acknowledgements We acknowledge the KAUST Machine Workshop, KAUST Electronics Workshop and G. D. Li for assistance in setting up the cooling and heating experiments, and L. Chen and B. Chew from KAUST Advanced Nanofabrication, Imaging and Characterization Core Lab facilities for assistance in AFM and SEM imaging characterization of the superhydrophobic coating.

Author Contributions I.U.V. conceived research and designed the experiments. I.U.V. and J.O.M. carried out the experiments. N.A.P., D.Y.C.C. and S.T.T. contributed with discussions, analysis and theoretical interpretation of the experimental results. I.U.V., D.Y.C.C. and N.A.P. wrote the manuscript. All authors edited the manuscript.

Author Information Reprints and permissions information is available at www.nature.com/reprints. The authors declare no competing financial interests. Readers are welcome to comment on the online version of the paper. Correspondence and requests for materials should be addressed to I.U.V. (ivanuriev.vakarelski@kaust.edu.sa) or N.A.P. (n-patankar@northwestern.edu).